Inflammation, Vol. 40, No. 4, August 2017 (© 2017)
DOI: 10.1007/s10753-017-0573-x

ORIGINAL ARTICLE

Salidroside Inhibits Inflammation Through PI3K/Akt/HIF Signaling After Focal Cerebral Ischemia in Rats

Yicong Wei,[1] Haimian Hong,[1] Xiaoqin Zhang,[1] Wenfang Lai,[1] Yingzheng Wang,[1] Kedan Chu,[1] John Brown,[1] Guizhu Hong,[1] and Lidian Chen[1,2]

Abstract—Salidroside is being investigated for its therapeutic potential in stroke because it is neuroprotective over an extended therapeutic window of time. In the present study, we investigated the mechanisms underlying the anti-inflammatory effects of salidroside (50 mg/kg intraperitoneally) in rats, given 1 h after reperfusion of a middle cerebral artery that had been occluded for 2 h. After 24 h, we found that salidroside increased the neuronal nuclear protein NeuN and reduced the marker of microglia and macrophages CD11b in the peri-infarct area of the brain. Salidroside also decreased IL-6, IL-1β, TNF-α, CD14, CD44, and iNOs mRNAs. At the same time, salidroside increased the ratio of phosphorylated protein kinase B (p-Akt) to total Akt. The phosphoinositide 3-kinase (PI3K) inhibitor LY294002 prevented this increase in p-Akt and reversed the inhibitory effects of salidroside on CD11b and inflammatory mediators. Salidroside also elevated the protein levels of hypoxia-inducible factor (HIF) subunits HIF1α, HIF2α, HIF3α, and of erythropoietin (EPO). The stimulatory effects of salidroside on HIFα subunits were blocked by LY294002. Moreover, YC-1, a HIF inhibitor, abolished salidroside-mediated increase of HIF1α and prevented the inhibitory effects of salidroside on CD11b and inflammatory mediators. Taken together, our results provide evidence for the first time that all three HIFα subunits and EPO can be regulated by PI3K/Akt in cerebral tissue, and that salidroside entrains this signaling pathway to induce production of HIFα subunits and EPO, one or more of which mediate the anti-inflammatory effects of salidroside after cerebral IRI.

KEY WORDS: cerebral ischemia; hypoxia-inducible factors; inflammation; phosphoinositide 3-kinase; salidroside.

INTRODUCTION

The inflammatory responses that occur soon after cerebral ischemia/reperfusion injury (IRI) are characterized by a rapid activation of resident pro-inflammatory cells, including microglia, followed by the infiltration of additional inflammatory cells from the circulation. These cells all exacerbate the inflammatory response, leading to increased brain edema and neuronal death [1, 2]. Blockade of inflammatory mediators, such as cluster of differentiation 44 (CD44) and inducible nitric oxide synthase (iNOS), by chemical or genetic means, ameliorates ischemic brain injury in experimental stroke [3, 4]. Thus, the potential of anti-inflammatory therapies to reduce ischemic brain damage has attracted considerable attention [5, 6].

The transcription factor hypoxia-inducible factors (HIFs) are heterodimers composed of an oxygen-dependent α subunit, namely HIF1α, HIF2α, and

Yicong Wei and Haimian Hong contributed equally to this work

[1] Center of Biomedical Research & Development, Fujian University of Traditional Chinese Medicine, No. 1 Huatou Road, Minhou Shangjie, Fuzhou, China

[2] To whom correspondence should be addressed at Center of Biomedical Research & Development, Fujian University of Traditional Chinese Medicine, No. 1 Huatou Road, Minhou Shangjie, Fuzhou, China. E-mail: cbr@fjtcm.edu.cn

the less understood HIF3α, and a constitutively expressed β subunit [7]. HIF1α and HIF2α are induced during hypoxia through a number of oxygen-sensing prolyl hydroxylases (PHDs), which hydroxylate HIFα subunits at conserved proline residues. This causes the HIFα subunits to bind to von Hippel–Lindau tumor suppressor protein (pVHL), marking the molecules for ubiquitination and degradation under normoxic conditions [8, 9]. Moreover, levels of HIF1α and HIF2α can be increased by the phosphoinositide 3-kinase (PI3K) pathway, in a PHD/pVHL-independent manner, under hypoxic conditions in non-cerebral cells [10–12]. The PI3K pathway is also associated with an increase of HIF1α in ischemic brain [13], but the effects of this pathway on HIF2α and HIF3α have not been investigated in the brain. In addition, a number of studies have demonstrated that increases of HIF1α can dampen inflammatory responses and reduce tissue damage in animal models of cerebral IRI [14–17], but whether changes in HIF2α and HIF3α are also involved in these anti-inflammatory effects remains largely unknown.

Salidroside [2-(4-hydroxyphenyl)ethyl-b-D-glucopyranoside, PubChem CID: 159278], a bioactive component of *Rhodiola rosea*, is being investigated for its therapeutic potential in stroke particularly because it is neuroprotective across a wide window of time in various models of ischemic stroke [18, 19]. The mechanisms by which salidroside has this neuroprotective effect are only now being dissected, and, although salidroside is known to modulate a variety of intracellular pathways that can reduce inflammation in some other disease models [18, 20–22], its effects on inflammatory signaling after cerebral IRI are poorly understood. We have previously reported that salidroside modulates early response genes after cerebral IRI [18], but whether salidroside modulates PI3K or any other intracellular second messengers in cerebral IRI is not known. Thus, for example, the effects of salidroside on HIFα subunits have not been investigated at all in the brain, although it has been reported that salidroside can induce HIF1α in renal fibroblastic and HepG2 cell lines [23]. Here, we investigate the potential link between the PI3K pathway and all three HIFα subunits in ischemic brain in response to salidroside treatment. We report, for the first time, that all three HIFα subunits can be regulated by PI3K/Akt in the brain, and that salidroside entrains this cerebral PI3K/Akt/HIFα signaling pathway to induce production of the three HIFα subunits, one or more of which mediate the anti-inflammatory effects of salidroside after cerebral IRI.

MATERIALS AND METHODS

Animals

All animal experiments were performed in accordance with the guidelines of the National Institutes of Health Guide for the care and use of laboratory animals and were approved by the Animal Care and Use Committee of Fujian University of Traditional Chinese Medicine.

Male Sprague-Dawley rats (weighting 220 ± 20 g) were purchased from Slac Laboratory Animal Co. Ltd. (Shanghai, China) and acclimatized to laboratory conditions (21–23 °C, 55–75% humidity, 12 h/12 h light/dark cycle), with free access to food and water, for 1 week before the experiments were started.

MCAO and Reperfusion in Rats

Middle cerebral artery occlusion (MCAO) and reperfusion in rats was conducted as described previously [18]. Briefly, the left common, internal, and external carotid arteries were exposed through a ventral cervical midline incision, and the left common and external carotid arteries were ligated with a suture. A microvascular clip was temporarily placed on the internal carotid artery, close to the left common carotid artery bifurcation, to allow introduction of a monofilament thread into the left common carotid artery. A suture was tightened around the left common carotid artery and the intraluminal monofilament thread, after which the microvascular clip was removed. The monofilament thread was advanced 20–22 mm from the carotid bifurcation along the internal carotid artery into the circle of Willis, to lodge in and occlude the origin of the left MCA. Reperfusion was induced by withdrawing the monofilament thread, after 2 h of occlusion. Sham animals were operated in the same manner except that a monofilament thread was not advanced to occlude the middle cerebral artery. A total of 100 animals were used in the study, 16 of which were excluded due to the peri-operative death of the animal (n = 9) or because they did not meet the criteria described below (n = 7).

Neurological Deficit Measurement and Drug Treatments

Neurological deficit scoring was performed by blinded observers, 1 and 24 h after reperfusion, according to the 5-point scale described previously [24]: 0, no neurological deficit; 1, failure to extend the left forepaw fully; 2, circling to the left; 3, unable to bear weight on the left side; and 4, no spontaneous walking and/or complete

immobility. MCAO/reperfusion rats with neurological deficit scores of 2–4 were randomly assigned to receive intraperitoneally injected vehicle (saline, n = 14) or 50 mg/kg salidroside (n = 14), injected 1 h after reperfusion. A sham-operated group was also injected with vehicle (n = 12). After 24 h, the animals were sacrificed, and their left cerebral hemispheres were dissected and frozen at −80 °C for protein and RNA extraction (n = 6–7 per group). For immunofluorescence staining (n = 5 per group), brains were perfusion-fixed with a mixture of 1:1:8 parts 40% formaldehyde:glacial acetic acid:methanol delivered under a constant pressure of 110 mmHg, then dissected and embedded in paraffin, as previously described [18, 25, 26].

To investigate the role of the PI3K/protein kinase B (Akt) pathway after cerebral IRI, LY294002 (Sigma-Aldrich), a selective PI3K inhibitor, was administrated to rats, as described previously with some modifications [27]. Briefly, further, animals with neurological deficit scores of 2–4 were randomly divided into two groups and intraperitoneally injected with vehicle or 50 mg/kg salidroside (n = 6–7) 1 h after MCAO with reperfusion. These animals had already received 10 μl of 10 mM LY294002 in 25% dimethyl sulfoxide (DMSO)/phosphate-buffered saline (PBS) or 10 μl 25% DMSO/PBS intracerebroventricularly (injected from bregma: anteroposterior, −0.9 mm; mediolateral, 1.5 mm; depth, 3.5 mm) 30 min before MCAO (n = 15 per group). After 24 h, the animals were sacrificed and their left cerebral hemispheres were removed and frozen at −80 °C for protein and for RNA extraction.

To investigate the role of HIF after cerebral IRI, 1 ml of the HIF inhibitor YC-1 at 2 mg/kg body weight (dissolved in 1% DMSO/PBS, Sigma-Aldrich) or vehicle (1% DMSO/PBS) was administrated through the femoral vein 30 min before MCAO, as described previously [28]. One hour after reperfusion, rats with neurological deficit scores of 2–4 were randomly assigned into two groups and injected intraperitoneally with vehicle or 50 mg/kg salidroside (n = 6–7 per group). After 24 h, the animals were sacrificed and their left cerebral hemispheres were removed and frozen at −80 °C.

qRT-PCR

Frozen brain tissues were homogenized using a mortar and pestle in the presence of liquid nitrogen. The samples were divided into two portions that were subsequently used for RNA and protein extraction. Total RNA extraction and qRT-PCR were performed as described previously [18]. Briefly, total RNA was extracted using RNeasy Mini Kit, according to the manufacturer's instructions (Qiagen, Hilden, Germany). First strand cDNAs were synthesized from total RNA using the Superscript First-Strand Synthesis System according to the manufacturer's instructions (Life Technologies, Grand Island, NY). PCR was carried out using SYBR Green real-time PCR master mix (Life Technologies), according to the manufacturer's instructions. GAPDH was used as an internal control. Results were expressed as fold change relative to MCAO control, after normalization to GAPDH. All primer sequences are available upon request.

Western Blot Analysis

Western blot analysis was performed as described previously with some modification [18]. Briefly, homogenized tissues were lysed in RIPA buffer (Beyotime, Jiang-Su, China) plus 1% PMSF (Beyotime) and 1% protease inhibitor cocktail (Sigma-Aldrich). Protein samples were separated by SDS-PAGE and probed with anti-phosphorylated Akt antibody (Ser473, 1:500; Cell Signaling Technology, Danvers, MA), or probed with anti-HIF1α antibody (1:500), anti-HIF2α antibody (1:500), and anti-HIF3α antibody (1:500) from Novus Biologicals (Littleton, CO), or anti-CD11b antibody (1:1000; Abcam, Cambridge, UK), or with anti-EPO antibody (1:500) and anti-Akt antibody (1:800) from Santa Cruz Biotechnology (Dallas, TX). The blots were stripped and re-probed with anti-β-actin antibody (1:1000; Beyotime). Blots were imaged and analyzed using a ChemiDoc XRS+ imaging system (Bio-Rad, Hercules, CA) and ImageJ software, respectively. The data are presented as fold changes relative to the MCAO group after normalized to β-actin.

Immunofluorescent Staining

The immunostaining was performed as described previously with some modifications [29]. Briefly, the coronal sections (10 μm) were cut at bregma −1 mm of the paraffin-embedded ischemic brain tissue using a microtome (Thermo Scientific HM325) and paraffin removed with xylene/ethanol. The tissues were subjected to antigen retrieval in 10 mM sodium citrate (pH 6.0) at 100 °C for 15 min and then incubated in 3% H_2O_2 for 10 min. The tissues were pre-incubated with the blocking solution (0.1% Triton X-100/2% normal goat serum in PBS) for 30 min at room temperature and incubated with rabbit polyclonal anti-CD11b antibody (1:100; Abcam) diluted in the blocking solution at 4 °C overnight, followed by incubation with TRITC-conjugated goat anti-Rabbit IgG (1:200) for 1 h at room temperature. Nuclei were

counterstained with DAPI (Beyotime). Sections were observed using a LSM 710 laser scanning confocal microscope (Carl Zeiss AG, Oberkochen, Germany), with 550 nm excitation light. Cells emitting red fluorescence at their cellular membrane were considered CD11b-positive. The number of CD11b-positive cells across five random visual fields at ×200 magnification in each section in the peri-infarct zone was recorded by an investigator blinded to the treatment. NeuN-positive cells were also examined in the brain by immunofluorescence using mouse monoclonal anti-NeuN antibody (1:1000; Abcam) and FITC-conjugated anti-mouse IgG (1:400) with 493 nm excitation light. Cells emitting green nuclear fluorescence were considered NeuN-positive. The number of NeuN-

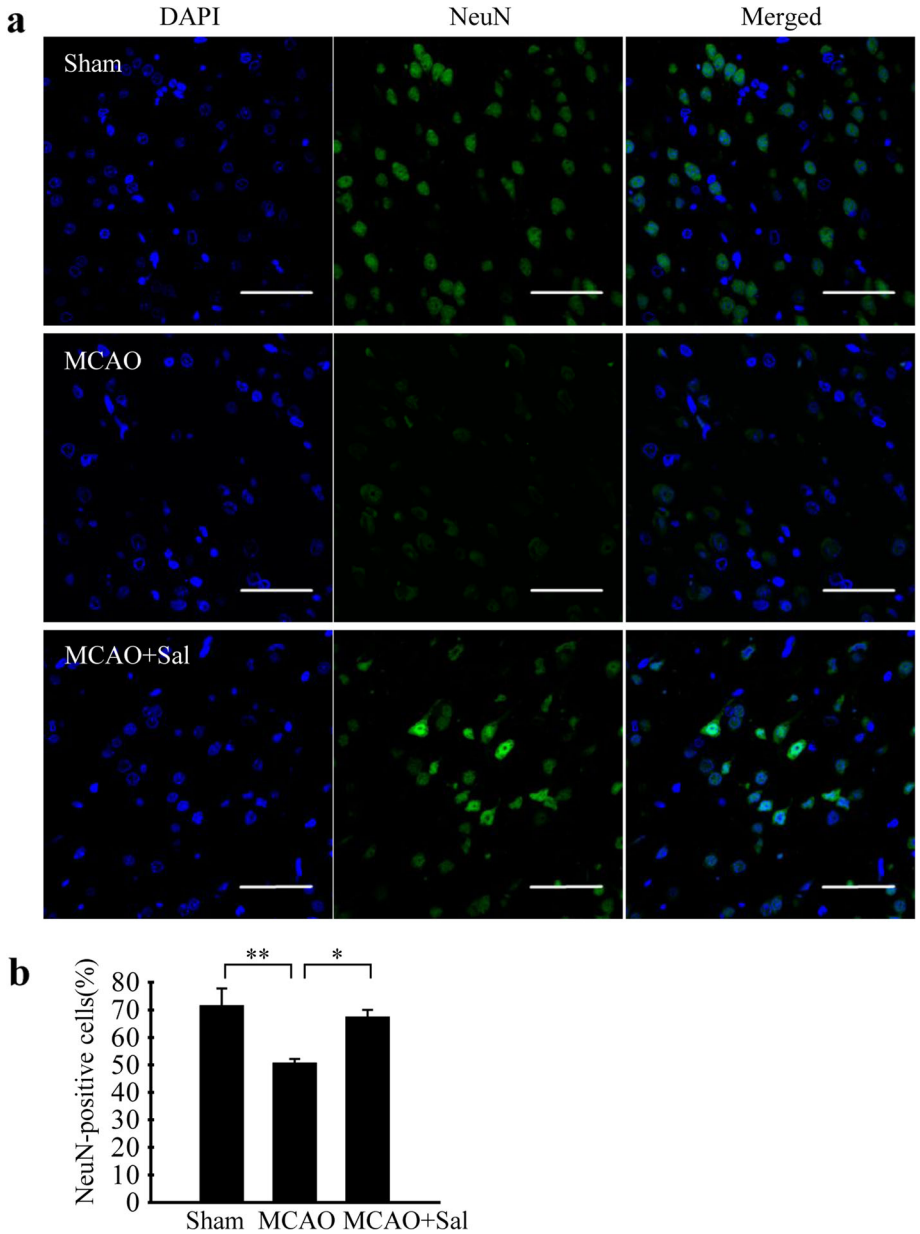

Fig. 1. Salidroside increases NeuN in the peri-infarct area of the brain after IRI. **a** Representative images showing NeuN staining in the peri-infarct zone of the MCAO and MCAO + salidroside groups, and the corresponding area for the sham-operated group. Merged images are an overlay of NeuN (*green*) and DAPI (*blue*) staining (magnification, ×400; *bar* = 50 μm). **b** The percentage of NeuN-positive cells to total cells in five random fields from the peri-infarct area (or, for sham-operated, the corresponding area) of each section. Data are means ± SEM ($n = 5$ per group). *$0.01 < p < 0.05$, **$p < 0.01$.

positive cells across five random visual fields at ×200 magnification in each section in the peri-infarct zone was recorded by an investigator blinded to the treatment. Data are presented as the mean percentage of CD11b- or NeuN-positive cells to total cells ± SEM (n = 5 per group).

Statistical Analysis

Results are presented as means ± SEM and analyzed using one-way ANOVA followed by multiple comparisons with post hoc Bonferroni test. A p value less than 0.05 was considered statistically significant.

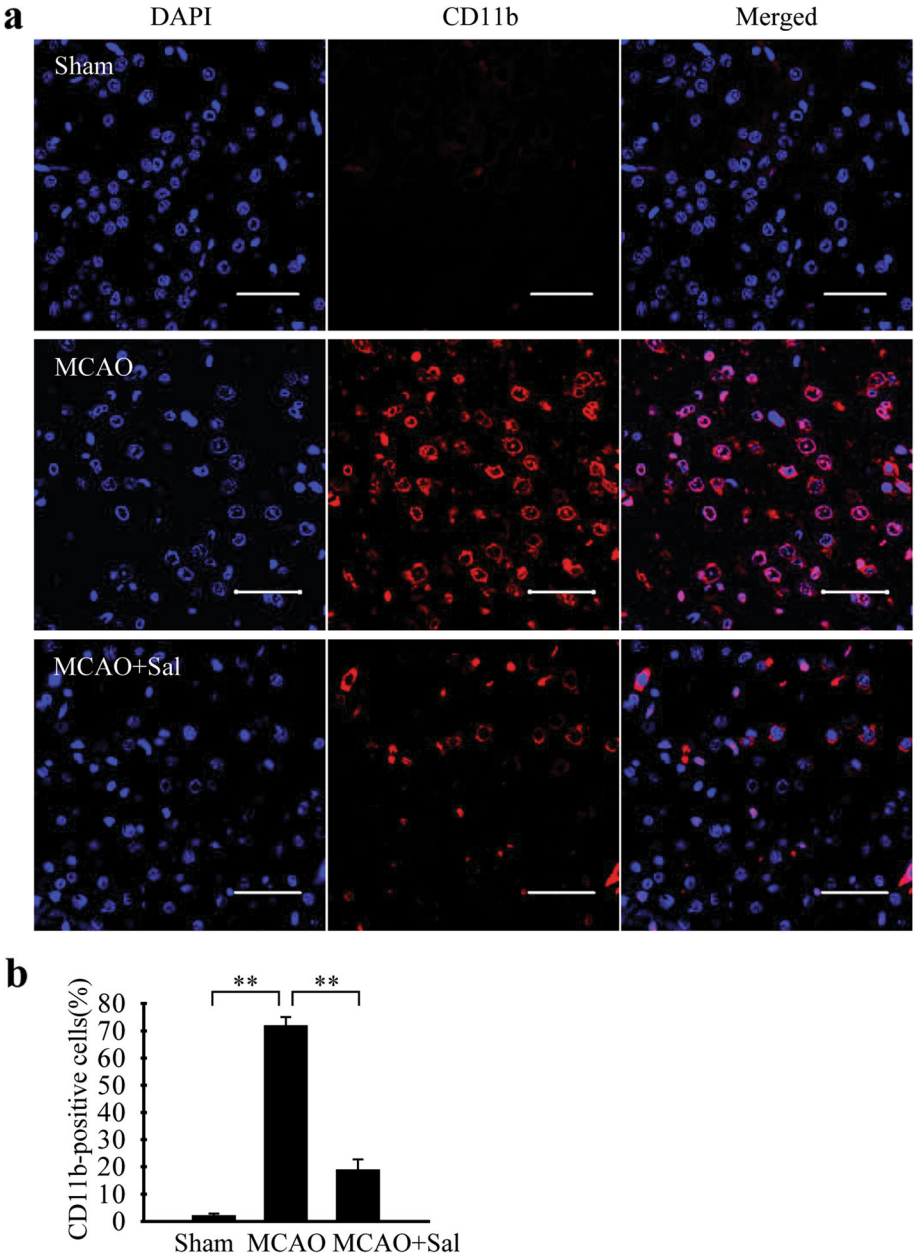

Fig. 2. Salidroside reduces CD11b in the peri-infarct area of the brain after IRI. **a** Representative images showing CD11b staining in the peri-infarct zone of the MCAO and MCAO + salidroside groups, and the corresponding area for the sham-operated group. Merged images are an overlay of CD11b (*red*) and DAPI (*blue*) staining (magnification, ×400; *bar* = 50 μm). **b** The percentage of CD11b-positive cells to total cells in five random fields from the peri-infarct area (or, for sham-operated, the corresponding area) of each section. Data are means ± SEM (n = 5 per group). $^{**}p < 0.01$.

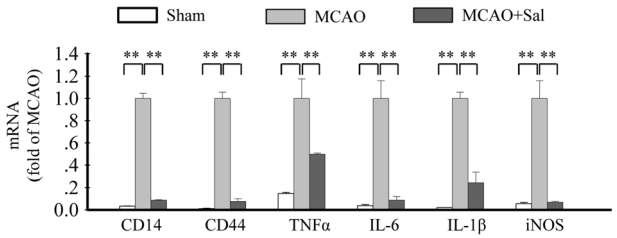

Fig. 3. Salidroside decreases CD14, CD44, TNF-α, IL-6, IL-1β, and iNOS mRNAs in ischemic brain. mRNA levels were measured by qRT-PCR and normalized to GAPDH. All values are expressed as mean fold changes relative to the MCAO group ± SEM ($n = 6$ per group). $^{**}p < 0.01$.

RESULTS

Salidroside Increases NeuN While Decreasing CD11b and Pro-inflammatory Mediators in the Brain After IRI

Immunofluorescence staining showed that salidroside prevented the decrease of the neuronal nuclear protein NeuN caused by IRI in the peri-infarct area of the brain after IRI (Fig. 1). At the same time, CD11b, a marker of activated microglia and macrophages [30], was dramatically increased in the peri-infarct area of the brain after IRI, compared to the corresponding area of sham operation, and this increase was prevented by salidroside (Fig. 2).

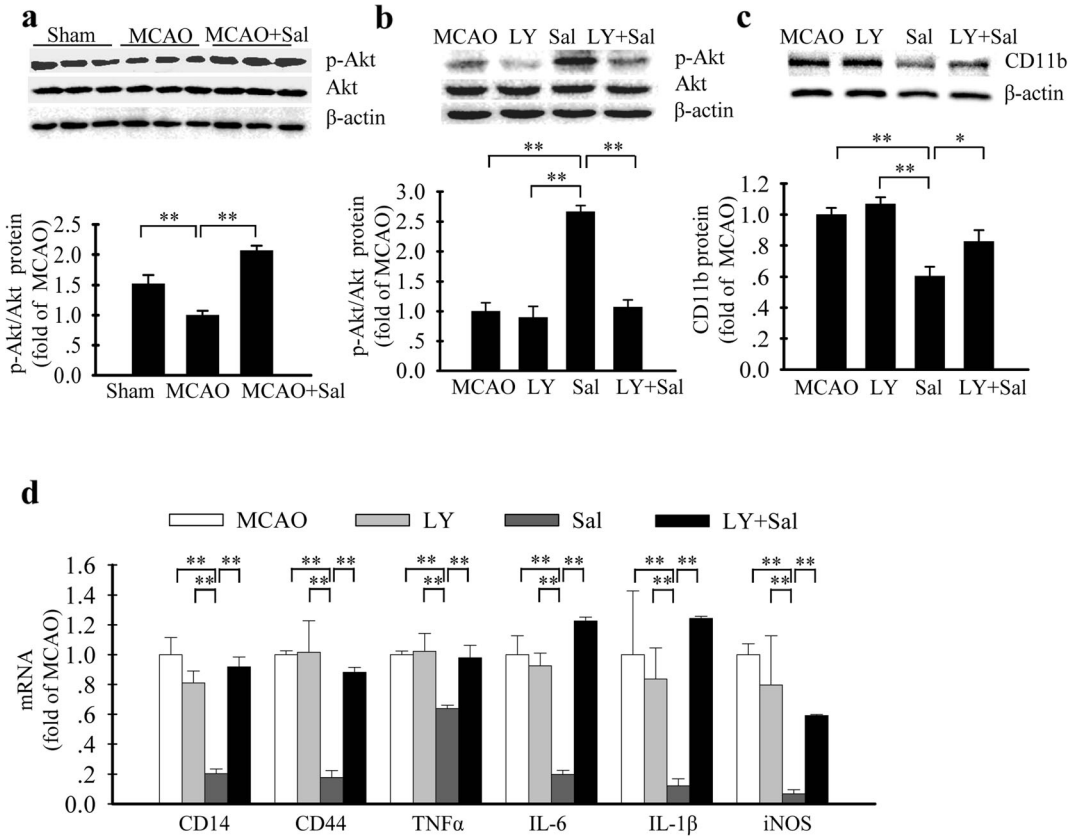

Fig. 4. Salidroside reduces inflammation involving in activation of PI3K/Akt in ischemic brain. **a** Salidroside increases the ratio of p-Akt to total Akt. A representative western blot probed with anti-p-Akt antibody, anti-Akt antibody, and anti-β-actin antibody is shown in the *upper panel*, and the ratio of p-Akt to total Akt, normalized to β-actin level, is shown in the *lower panel*. **b** LY294002 abolishes salidroside-mediated increase of the ratio of p-Akt to total Akt. A representative western blot probed with anti-p-Akt antibody, anti-Akt antibody, and anti-β-actin antibody is shown in the *upper panel*, and the ratio of p-Akt to total Akt, normalized to β-actin level, is shown in the *lower panel*. **c** LY294002 reverses salidroside-mediated inhibition of CD11b. A representative western blot probed with anti-CD11b antibody and anti-β-actin antibody is shown in the *upper panel*, and CD11b protein level, normalized to β-actin level, is shown in the *lower panel*. **d** LY294002 reverses salidroside-mediated inhibition of CD14, CD44, TNF-α, IL-6, IL-1β, and iNOS mRNAs. The mRNA levels were measured by qRT-PCR and normalized to the level of GAPDH mRNA. All values are expressed as mean fold changes relative to the MCAO group ± SEM ($n = 6$ per group). $^{*}0.01 < p < 0.05$, $^{**}p < 0.01$.

RT-PCR technique was used to measure the messenger RNA (mRNA) levels of pro-inflammatory cytokines and mediators. As shown in Fig. 3, CD14, CD44, TNF-α, IL-6, IL-1β, and iNOS mRNAs were all significantly increased in the brain after IRI, compared to the sham-operated group, and these increases were abolished by administration of salidroside.

Salidroside Reduces Inflammation by Activating PI3K/Akt Signaling

Activation of PI3K/Akt signaling can reduce pro-inflammatory responses in a variety of cell types [31–34]. We therefore investigated whether the PI3K/Akt pathway was involved in the action of salidroside to inhibit cerebral inflammation. The ratio of p-Akt to total Akt was decreased in the brain after IRI compared to the sham-operated group. This decrease was prevented by salidroside treatment (Fig. 4a). LY294002, a selective inhibitor of PI3K, abolished the increase in the ratio of p-Akt/Akt caused by salidroside (Fig. 4b). LY294002 also prevented the inhibitory effects of salidroside on the protein level of CD11b and the mRNA levels of IL-6, IL-1β, TNF-α, CD14, CD44, and iNOS (Fig. 4c, d). LY294002 given alone had no significant effect on these protein and mRNA levels.

Salidroside Activation of PI3K/Akt Signaling Leads to Increase in HIF

We then investigated the effects of the activation of PI3K/Akt signaling by salidroside on cerebral HIFs after IRI. IRI significantly reduced the protein levels of HIF1α, HIF2α, and HIF3α. Treatment with salidroside prevented all these decreased HIF protein levels (Fig. 5a–c). Additionally, we measured the protein level of erythropoietin (EPO), a downstream target of HIF, in the brain after IRI. EPO was reduced by IRI and this decrease was prevented by salidroside (Fig. 5d).

To investigate whether the PI3K/Akt pathway was associated with the increase of HIF caused by salidroside, we administrated vehicle, salidroside, LY294002, or the combination of salidroside and LY294002 to animals after IRI. LY294002 given alone had no effect of the

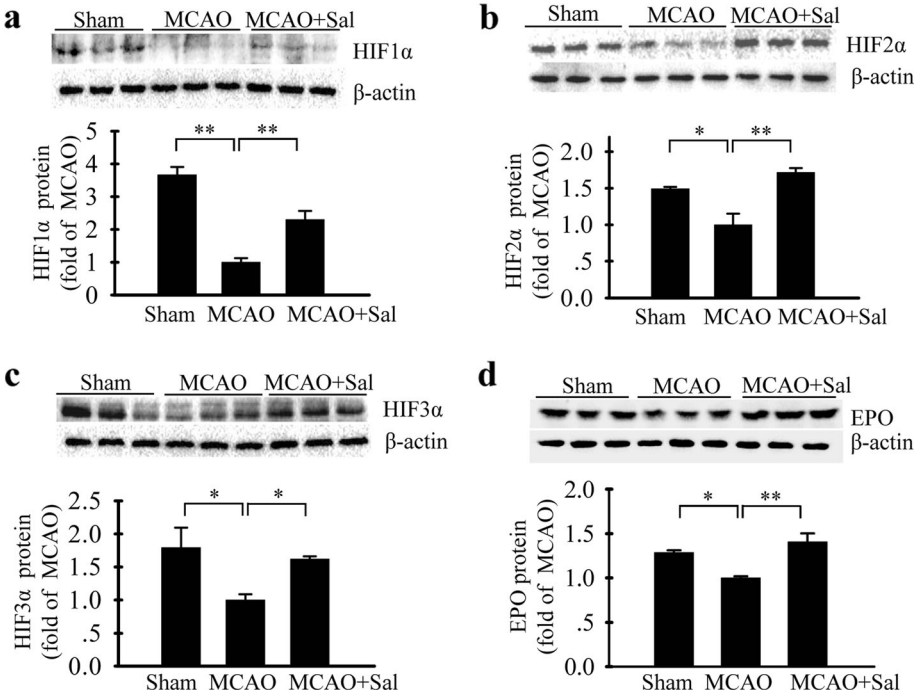

Fig. 5. Salidroside increases the protein levels of HIF and EPO in the brain after IRI. **a** A representative western blot probed with anti-HIF1α antibody and anti-β-actin antibody (*upper panel*), and HIF1α protein level normalized to β-actin (*lower panel*). **b** A representative western blot probed with anti-HIF2α antibody and anti-β-actin antibody (*upper panel*), and HIF2α protein level normalized to β-actin (*lower panel*). **c** A representative western blot probed with anti-HIF3α antibody and anti-β-actin antibody (*upper panel*), and HIF3α protein level normalized to β-actin (*lower panel*). **d** A representative western blot probed with anti-EPO antibody and anti-β-actin antibody (*upper panel*), and EPO protein level normalized to β-actin (*lower panel*). All values are expressed as mean fold changes relative to the MCAO group ± SEM ($n = 6$ per group). *$0.01 < p < 0.05$, **$p < 0.01$.

levels of HIFα subunits, but we found that salidroside increased the protein levels of HIF1α, HIF2α, and HIF3α after cerebral IRI and these increases could be blocked by LY294002 (Fig. 6a–c). Neither salidroside nor LY294002 given alone affected the mRNA levels of HIF1α and HIF2α. On the other hand, salidroside alone significantly induced HIF3α mRNA. LY294002 given alone did not affect the level of HIF3α mRNA but could abolish the increase in HIF3α mRNA caused by salidroside (Fig. 6d).

Increase of HIF Mediates the Anti-inflammatory Effect of Salidroside

To confirm further the involvement of HIFs in the salidroside-mediated inhibition of inflammation, we administrated YC-1, an inhibitor of HIF [35, 36], along with salidroside. As expected, YC-1 reversed increase of HIF1α caused by salidroside (Fig. 7a). YC-1 also abolished the inhibitory effects of salidroside on CD11b and inflammatory mediators (Fig. 7b, c).

DISCUSSION

Previous work has implicated an effect of salidroside on PI3K/Akt signaling in protecting cultured PC12 cells [37], and in maintaining neuronal number in a Drosophila model of Alzheimer's disease [38], in experimental traumatic brain injury [39], and in a mouse model of Parkinson's disease [40]. However, salidroside is being investigated as a promising potential therapeutic agent for ischemic stroke because it is neuroprotective across a wide therapeutic time window in experimental stroke models [18, 19]. Our findings are the first investigation of the effects of salidroside on PI3K and HIFs in an animal model of ischemic stroke. Moreover, the involvement of a PI3K/HIF signaling pathway in anti-inflammatory effects of salidroside after cerebral IRI has not previously been investigated. This is important because there is already data that salidroside may engage different anti-inflammatory mechanisms in different disease states and tissues. For example, salidroside is anti-inflammatory in murine endotoxemia by blocking NF- B

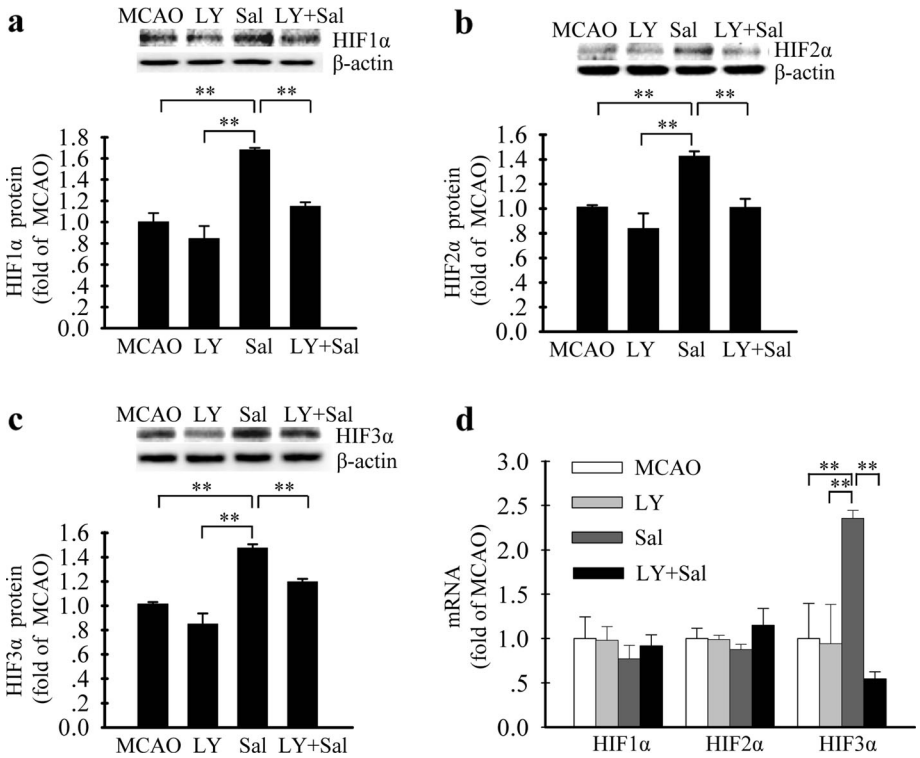

Fig. 6. Effects of salidroside-mediated activation of PI3K/Akt on HIFα subunits. **a**–**c** Salidroside increases the protein levels of HIF1α (**a**), HIF2α (**b**), and HIF3α (**c**), and these stimulatory effects are abolished by LY294002. Representative western blots probed with anti-HIF1α antibody (**a**), anti-HIF2α antibody (**b**), anti-HIF3α antibody (**c**), and anti-β-actin antibody are shown in the *upper panels*, and the protein levels of HIF1α (**a**), HIF2α (**b**), and HIF3α (**c**) normalized to β-actin are shown in the *lower panels*. **d** Effects of salidroside and LY294002 on HIF mRNAs. The mRNA levels were measured by qRT-PCR and normalized to GAPDH mRNA. All values are expressed as mean fold changes relative to the MCAO group ± SEM ($n = 6$ per group). $^{**}p < 0.01$.

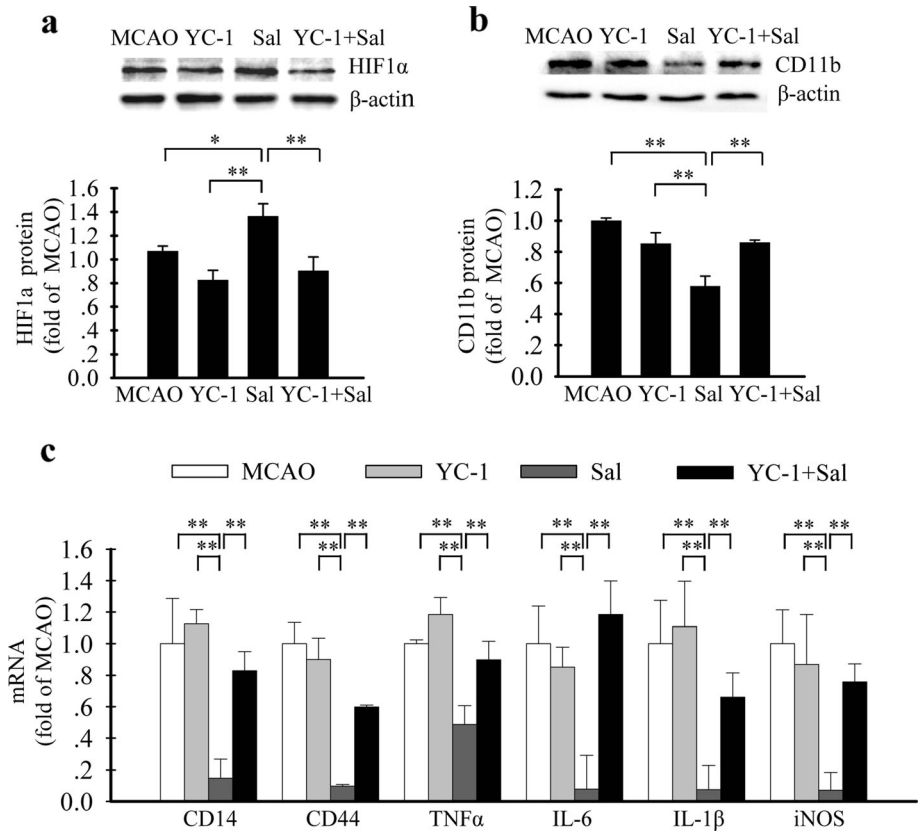

Fig. 7. YC-1 abolishes the effects of salidroside on HIF1α, CD11b and pro-inflammatory cytokines. **a**, **b** YC-1 abolishes the effects of salidroside on the protein levels of HIF1α (**a**) and CD11b (**b**). Representative western blots probed with anti-HIF1α antibody (**a**), anti-CD11b antibody (**b**), and anti-β-actin antibody (*upper panels*). HIF1α (**a**) and CD11b (**b**) protein levels normalized to β-actin (*lower panels*). **c** YC-1 abolishes the inhibitory effects of salidroside on pro-inflammatory cytokines. The mRNA levels were measured by qRT-PCR and normalized to GAPDH mRNA. All values are expressed as mean fold changes relative to the MCAO group ± SEM ($n = 6$ per group). *$0.01 < p < 0.05$, **$p < 0.01$.

and ERK/MAPKs [41], it is anti-inflammatory in isoproterenol-induced myocardial injury *via* regulation of Nox/NF-κB/AP1 [20], it attenuates lipopolysaccharide-induced serum cytokines in mice through the BDNF/TrkB pathway [42], it suppresses inflammation in a D-galactose-induced rat model of Alzheimer's disease *via* the SIRT1/NF-κB pathway [22], it suppresses ultraviolet-induced skin inflammation by targeting cyclooxygenase-2 [43], and it regulates the inflammatory response in Raw 264.7 macrophages *via* TLR4/TAK1 [44]. In the present study, we showed that salidroside increased the ratio of p-Akt to total Akt and prevented the increased CD11b and pro-inflammatory mediators after cerebral IRI. All these effects of salidroside were reversed by the PI3K inhibitor LY294002. Thus, we provide evidence, for the first time, that salidroside significantly inhibits inflammation in experimental stroke through activation of the PI3K/Akt pathway.

HIF1α mediates several of the early protective responses to hypoxia and IRI in cerebral tissues and has been proposed as a therapeutic target for stroke [15, 16]. However, there is less information on the roles of HIF2α and HIF3α in cerebral IRI. It has been previously reported that PI3K/Akt signaling can induce HIF1α at the stage of protein synthesis through a PI3K/Akt/mTOR pathway in a retinal pigmentary epithelial cell line and in prostatic cancer cells [12, 45] and by protecting HIF1α from PDHs/pVHL-independent degradation *via* increase of heat shock proteins in renal carcinoma cells [11], while a macrophage-preponderant isoform of PI3K is known to modulate the proteosomal degradation of HIF1α and HIF2α in macrophages [10]. The PI3K pathway is also associated with increase of HIF1α in ischemic brain [13], but the control of HIF2α and HIF3α by PI3K/Akt has not previously been investigated in the brain cells either *in vitro* or *in vivo*. In the present study, we did not find

any significant effect of the PI3K inhibitor LY294002 given alone on the expression of HIFα subunits after IRI. However, salidroside triggered a PI3K/Akt pathway to increase HIFs after IRI. Thus, we found that salidroside induced the protein levels of HIF1α, HIF2α, and HIF3α subunits in the brain after IRI. All these stimulatory effects of salidroside were reversed by LY294002, suggesting that the PI3K/Akt pathway mediates the regulation of all three HIFα subunits by salidroside after cerebral IRI. Nothing had previously been known of the effects of salidroside on cerebral HIFs, although salidroside has been found to increase HIF1α, but not HIF2α, in renal fibroblastic and HepG2 cell lines [23]. We further found that salidroside induced cerebral HIF3α mRNA after IRI and that this increase was blocked by LY294002. However, neither salidroside nor LY294002, either alone or in combination, affected HIF1α and HIF2α mRNA levels after cerebral IRI, suggesting that the PI3K/Akt pathway triggered by salidroside after cerebral IRI increases only HIF3α at the transcriptional level. Additionally, we have observed that neither salidroside nor LY294002 altered the mRNA levels of PDH1, PDH2, PDH3, and pVHL (data not shown), consistent with the idea that the increases of HIF1α and HIF2α caused by activation of PI3K were independent of the PDHs/HIF/pVHL axis, which is otherwise a prominent regulator of HIF degradation and HIF levels [46]. The mechanisms underlying PI3K/Akt signaling regulation of HIFα subunits in the brain require further investigation, although one possibility is that, as in prostatic carcinoma cells, Akt can control HIF1α at the translational levels through a pathway involving mTOR and 4E-BP [45]. Nevertheless, we provide evidence, for the first time, that the PI3K/Akt signaling induces all three HIFα subunits in ischemic brain, that the mechanism downstream of PI3K/Akt that regulates HIF1α and HIF2α differs from that regulating HIF3α, and that salidroside entrains cerebral PI3K/Akt to induce production of all three HIFα subunits.

In addition, we found that YC-1, an inhibitor of HIF1α and HIF2α [35, 36, 45], blocked the inhibitory effects of salidroside on CD11b and pro-inflammatory mediators. The effects of YC-1 on HIF3α are less well documented. Nevertheless, our results with the protein expression of HIFs and with YC-1 are consistent with the hypothesis that increased activity of HIF1α and HIF2α significantly mediates the anti-inflammatory effects of salidroside in ischemic brain. Recent studies have shown that HIF3α can act as an oxygen-dependent transcription factor in response to hypoxia, with some effects similar to those of HIF1α and HIF2α [47, 48]. It is possible, therefore, that the increase in HIF3α caused by salidroside is also involved in reducing inflammatory mediators. Taken together, our results suggest that the increase in HIFα subunits mediated by salidroside contributes to the anti-inflammatory actions of salidroside in ischemic brain.

Our findings in the present study are consistent with previous reports showing that HIF1α is associated with the anti-inflammatory effects of several neuroprotective agents in ischemic brain [17, 49]. In contrast, Koh *et al.* [50] have reported that HIF1α is involved in the inflammatory brain damage mediated through TIM3 in a mouse cerebral hypoxia–ischemia model. One explanation for this discrepancy is that different experimental models were used, with myeloid-specific HIF1α-deficient mice used in the study by Koh *et al.*, whereas acute pharmacological inhibition of HIF1α was used in the present and other studies.

Whether salidroside directly targeted microglia and decreased their pro-inflammatory cytokine mRNAs in our model of IRI remains to be investigated. Our results with CD11b suggest that salidroside reduced the number of activated microglia and/or macrophages. We have previously shown that salidroside reduces the LPS-induced mobility of BV2 microglial cells [21]. These results suggest that salidroside could directly act on microglial cells. However, salidroside-mediated inhibition of inflammation may also have been secondary to enhanced neuronal survival driven by salidroside-stimulated EPO production, a downstream

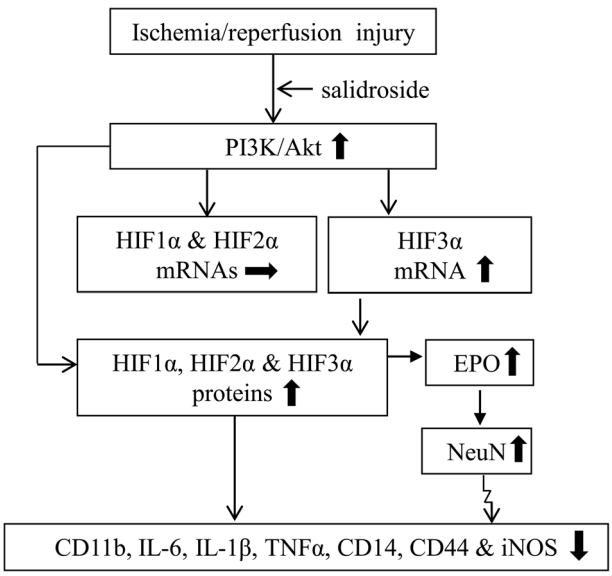

Fig. 8. A schematic diagram illustrating the probable anti-inflammatory actions of salidroside in the brain after IRI. *Bold arrows* indicate the direction of the effects of salidroside in inhibiting or increasing intermediate mediators.

target of HIF that exhibits neuroprotective and anti-inflammatory activities [51]. Salidroside treatment certainly enhanced neuronal survival in the present study, as evinced by the increase it caused in NeuN immunoreactivity. EPO is primarily synthesized in astrocytes [52, 53], although neurons can also produce EPO, and both neurons and glia express EPOR [54]. This range of cell types producing EPO and EPOR means the underlying molecular mechanisms of the cerebral effects of HIF/EPO can be complex and may be paracrine and possibly also autocrine. The precise intercellular relationships therefore remain to be investigated, but, in conclusion, the present study provides evidence for the first time that all three HIFα subunits and EPO can be regulated by PI3K/Akt in cerebral tissue, and that salidroside entrains this signaling pathway to induce production of HIFα subunits and EPO, one or more of which mediate the anti-inflammatory effects of salidroside after cerebral IRI, as summarized in Fig. 8.

ACKNOWLEDGMENTS

This work was supported by the National Natural Science Foundation of China (Grant No. 81473382), the Department of Technology and Science and the Department of Health of Fujian Provincial Government (Grant Nos. 2014Y4004 and WZZY201305), the Collaborative Innovation Center for Rehabilitation Technology of Fujian University of TCM, and the TCM Rehabilitation Research Center of SATCM. The authors would like to acknowledge the staff of the Animal Centre of the Fujian University of TCM for their excellent technical support.

COMPLIANCE WITH ETHICAL STANDARDS

Conflict of Interest. The authors declare that they have no competing interests.

REFERENCES

1. Jin, R., G. Yang, and G. Li. 2010. Inflammatory mechanisms in ischemic stroke: role of inflammatory cells. *Journal of Leukocyte Biology* 87: 779–789.
2. Hallenbeck, J.M. 1997. Cytokines, macrophages, and leukocytes in brain ischemia. *Neurology* 49: S5–S9.
3. Han, H.S., Y. Qiao, M. Karabiyikoglu, R.G. Giffard, and M.A. Yenari. 2002. Influence of mild hypothermia on inducible nitric oxide synthase expression and reactive nitrogen production in experimental stroke and inflammation. *Journal of Neuroscience* 22: 3921–3928.
4. Wang, X., L. Xu, H. Wang, Y. Zhan, E. Pure, and G.Z. Feuerstein. 2002. CD44 deficiency in mice protects brain from cerebral ischemia injury. *Journal of Neurochemistry* 83: 1172–1179.
5. Muresanu, D.F., A. Buzoianu, S.I. Florian, and T. von Wild. 2012. Towards a roadmap in brain protection and recovery. *Journal of Cellular and Molecular Medicine* 16: 2861–2871.
6. Zhang, W. and D. Stanimirovic. 2002. Current and future therapeutic strategies to target inflammation in stroke. *Current Drug Targets. Inflammation and Allergy* 1: 151–166.
7. Greer, S.N., J.L. Metcalf, Y. Wang, and M. Ohh. 2012. The updated biology of hypoxia-inducible factor. *EMBO Journal* 31: 2448–2460.
8. Weidemann, A., and R.S. Johnson. 2008. Biology of HIF-1alpha. *Cell Death and Differentiation* 15: 621–627.
9. Maxwell, P.H., M.S. Wiesener, G.W. Chang, S.C. Clifford, E.C. Vaux, M.E. Cockman, C.C. Wykoff, C.W. Pugh, E.R. Maher, and P.J. Ratcliffe. 1999. The tumour suppressor protein VHL targets hypoxia-inducible factors for oxygen-dependent proteolysis. *Nature* 399: 271–275.
10. Joshi, S., A.R. Singh, M. Zulcic, and D.L. Durden. 2014. A macrophage-dominant PI3K isoform controls hypoxia-induced HIF1 and HIF2 stability and tumor growth, angiogenesis, and metastasis. *Molecular Cancer Research* 12: 1520–1531.
11. Zhou, J., T. Schmid, R. Frank, and B. Brune. 2004. PI3K/Akt is required for heat shock proteins to protect hypoxia-inducible factor 1alpha from pVHL-independent degradation. *Journal of Biological Chemistry* 279: 13506–13513.
12. Treins, C., S. Giorgetti-Peraldi, J. Murdaca, G.L. Semenza, and E. Van Obberghen. 2002. Insulin stimulates hypoxia-inducible factor 1 through a phosphatidylinositol 3-kinase/target of rapamycin-dependent signaling pathway. *Journal of Biological Chemistry* 277: 27975–27981.
13. Ye, Z., Q. Guo, P. Xia, N. Wang, E. Wang, and Y. Yuan. 2012. Sevoflurane postconditioning involves an up-regulation of HIF-1alpha and HO-1 expression via PI3K/Akt pathway in a rat model of focal cerebral ischemia. *Brain Research* 1463: 63–74.
14. Eltzschig, H.K., D.L. Bratton, and S.P. Colgan. 2014. Targeting hypoxia signalling for the treatment of ischaemic and inflammatory diseases. *Nature Reviews Drug Discovery* 13: 852–869.
15. Baranova, O., L.F. Miranda, P. Pichiule, I. Dragatsis, R.S. Johnson, and J.C. Chavez. 2007. Neuron-specific inactivation of the hypoxia inducible factor 1 increases brain injury in a mouse model of transient focal cerebral ischemia. *Journal of Neuroscience* 27: 6320–6332.
16. Shi, H. 2009. Hypoxia inducible factor 1 as a therapeutic target in ischemic stroke. *Current Medicinal Chemistry* 16: 4593–4600.
17. Wang, C., Z. Wang, X. Zhang, X. Zhang, L. Dong, Y. Xing, Y. Li, Z. Liu, L. Chen, H. Qiao, L. Wang, and C. Zhu. 2012. Protection by silibinin against experimental ischemic stroke: up-regulated pAkt, pmTOR, HIF-1α and Bcl-2, down-regulated Bax, NF-κB expression. *Neuroscience Letters* 529: 45–50.
18. Lai, W.F., Z.W. Zheng, X.Q. Zhang, Y.C. Wei, K.D. Chu, J. Brown, G.Z. Hong, and L.D. Chen. 2015. Salidroside-mediated neuroprotection is associated with induction of early growth response genes (Egrs) across a wide therapeutic window. *Neurotoxicity Research* 28: 108–121.
19. Shi, T.Y., S.F. Feng, J.H. Xing, Y.M. Wu, X.Q. Li, N. Zhang, Z. Tian, S.B. Liu, and M.G. Zhao. 2012. Neuroprotective effects of salidroside and its analogue tyrosol galactoside against focal cerebral ischemia *in vivo* and H_2O_2-induced neurotoxicity *in vitro*. *Neurotoxicity Research* 21: 358–367.

20. Zhu, L., T. Wei, X. Chang, H. He, J. Gao, Z. Wen, and T. Yan. 2015. Effects of salidroside on myocardial injury *in vivo in vitro* via regulation of Nox/NF-kappaB/AP1 pathway. *Inflammation* 38: 1589–1598.
21. Hu, H., Z. Li, X. Zhu, R. Lin, and L. Chen. 2014. Salidroside reduces cell mobility via NF-κB and MAPK signaling in LPS-induced BV2 microglial cells. *Evidence-based Complementary and Alternative Medicine* 2014: 383821.
22. Gao, J., R. Zhou, X. You, F. Luo, H. He, X. Chang, L. Zhu, X. Ding, and T. Yan. 2016. Salidroside suppresses inflammation in a D-galactose-induced rat model of Alzheimer's disease via SIRT1/NF-kappaB pathway. *Metabolic Brain Disease* 31: 771–778.
23. Zheng, K.Y., Z.X. Zhang, A.J. Guo, C.W. Bi, K.Y. Zhu, S.L. Xu, J.Y. Zhan, D.T. Lau, T.T. Dong, R.C. Choi, and K.W. Tsim. 2012. Salidroside stimulates the accumulation of HIF-1alpha protein resulted in the induction of EPO expression: a signaling via blocking the degradation pathway in kidney and liver cells. *European Journal of Pharmacology* 679: 34–39.
24. Longa, E.Z., P.R. Weinstein, S. Carlson, and R. Cummins. 1989. Reversible middle cerebral artery occlusion without craniectomy in rats. *Stroke* 20: 84–91.
25. Nakayama, H., M.D. Ginsberg, and W.D. Dietrich. 1988. (S)-emopamil, a novel calcium channel blocker and serotonin S2 antagonist, markedly reduces infarct size following middle cerebral artery occlusion in the rat. *Neurology* 38: 1667–1673.
26. Belayev, L., O.F. Alonso, R. Busto, W. Zhao, and M.D. Ginsberg. 1996. Middle cerebral artery occlusion in the rat by intraluminal suture. *Neurological and pathological evaluation of an improved model. Stroke* 27 (1616–1622): 1623.
27. Zhao, H., T. Shimohata, J.Q. Wang, G. Sun, D.W. Schaal, R.M. Sapolsky, and G.K. Steinberg. 2005. Akt contributes to neuroprotection by hypothermia against cerebral ischemia in rats. *Journal of Neuroscience* 25: 9794–9806.
28. Zhang, Z., J. Yan, S. Taheri, K.J. Liu, and H. Shi. 2014. Hypoxia-inducible factor 1 contributes to N-acetylcysteine's protection in stroke. *Free Radical Biology and Medicine* 68: 8–21.
29. Sun, M., B. Deng, X. Zhao, C. Gao, L. Yang, H. Zhao, D. Yu, F. Zhang, L. Xu, L. Chen, and X. Sun. 2015. Isoflurane preconditioning provides neuroprotection against stroke by regulating the expression of the TLR4 signalling pathway to alleviate microglial activation. *Scientific Reports* 5: 11445.
30. Perego, C., S. Fumagalli, and M.G. De Simoni. 2011. Temporal pattern of expression and colocalization of microglia/macrophage phenotype markers following brain ischemic injury in mice. *Journal of Neuroinflammation* 8: 174.
31. Guha, M., and N. Mackman. 2002. The phosphatidylinositol 3-kinase-Akt pathway limits lipopolysaccharide activation of signaling pathways and expression of inflammatory mediators in human monocytic cells. *Journal of Biological Chemistry* 277: 32124–32132.
32. Jin, R., Z. Song, S. Yu, A. Piazza, A. Nanda, J.M. Penninger, D.N. Granger, and G. Li. 2011. Phosphatidylinositol-3-kinase gamma plays a central role in blood-brain barrier dysfunction in acute experimental stroke. *Stroke* 42: 2033–2044.
33. Lai, W.F., X. Tian, Q. Xiang, K.D. Chu, Y. Wei, J.T. Deng, S.P. Zhang, J. Brown, and G.Z. Hong. 2015. 11β-HSD1 modulates LPS-induced innate immune responses in adipocytes by altering expression of PTEN. *Molecular Endocrinology* 29: 558–570.
34. Li, L., D.W. McBride, D. Doycheva, B.J. Dixon, P.R. Krafft, J.H. Zhang, and J.P. Tang. 2015. G-CSF attenuates neuroinflammation and stabilizes the blood–brain barrier via the PI3K/Akt/GSK-3β signaling pathway following neonatal hypoxia-ischemia in rats. *Experimental Neurology* 272: 135–144.
35. Chun, Y.S., E.J. Yeo, E. Choi, C.M. Teng, J.M. Bae, M.S. Kim, and J.W. Park. 2001. Inhibitory effect of YC-1 on the hypoxic induction of erythropoietin and vascular endothelial growth factor in Hep3B cells. *Biochemical Pharmacology* 61: 947–954.
36. Li, S.H., D.H. Shin, Y.S. Chun, M.K. Lee, M.S. Kim, and J.W. Park. 2008. A novel mode of action of YC-1 in HIF inhibition: stimulation of FIH-dependent p300 dissociation from HIF-1. *Molecular Cancer Therapeutics* 7: 3729–3738.
37. Zhang, L., W. Ding, H. Sun, Q. Zhou, J. Huang, X. Li, Y. Xie, and J. Chen. 2012. Salidroside protects PC12 cells from MPP(+)-induced apoptosis via activation of the PI3K/Akt pathway. *Food and Chemical Toxicology* 50: 2591–2597.
38. Zhang, B., Y. Wang, H. Li, R. Xiong, Z. Zhao, X. Chu, Q. Li, S. Sun, and S. Chen. 2016. Neuroprotective effects of salidroside through PI3K/Akt pathway activation in Alzheimer's disease models. *Drug Design, Development and Therapy* 10: 1335–1343.
39. Chen, S.F., H.J. Tsai, T.H. Hung, C.C. Chen, C.Y. Lee, C.H. Wu, P.Y. Wang, and N.C. Liao. 2012. Salidroside improves behavioral and histological outcomes and reduces apoptosis via PI3K/Akt signaling after experimental traumatic brain injury. *PloS One* 7: e45763.
40. Zhang, W., H. He, H. Song, J. Zhao, T. Li, L. Wu, X. Zhang, and J. Chen. 2016. Neuroprotective effects of salidroside in the MPTP mouse model of Parkinson's disease: involvement of the PI3K/Akt/GSK3beta pathway. *Parkinson's Disease* 2016: 9450137.
41. Guan, S., H. Feng, B. Song, W. Guo, Y. Xiong, G. Huang, W. Zhong, M. Huo, N. Chen, J. Lu, and X. Deng. 2011. Salidroside attenuates LPS-induced pro-inflammatory cytokine responses and improves survival in murine endotoxemia. *International Immunopharmacology* 11: 2194–2199.
42. Zhu, L., T. Wei, J. Gao, X. Chang, H. He, M. Miao, and T. Yan. 2015. Salidroside attenuates lipopolysaccharide (LPS) induced serum cytokines and depressive-like behavior in mice. *Neuroscience Letters* 606: 1–6.
43. Wu, D., P. Yuan, C. Ke, H. Xiong, J. Chen, J. Guo, M. Lu, Y. Ding, X. Fan, Q. Duan, F. Shi, and F. Zhu. 2016. Salidroside suppresses solar ultraviolet-induced skin inflammation by targeting cyclooxygenase-2. *Oncotarget* 7: 25971–25982.
44. Sun, P., S.Z. Song, S. Jiang, X. Li, Y.L. Yao, Y.L. Wu, L.H. Lian, J.X. Nan. 2016. Salidroside regulates inflammatory response in Raw 264.7 macrophages via TLR4/TAK1 and ameliorates inflammation in alcohol binge drinking-induced liver injury. *Molecules* 21:E 1490.
45. Sun, H.L., Y.N. Liu, Y.T. Huang, S.L. Pan, D.Y. Huang, J.H. Guh, F.Y. Lee, S.C. Kuo, and C.M. Teng. 2007. YC-1 inhibits HIF-1 expression in prostate cancer cells: contribution of Akt/NF-kappaB signaling to HIF-1alpha accumulation during hypoxia. *Oncogene* 26: 3941–3951.
46. Ivan, M., K. Kondo, H. Yang, W. Kim, J. Valiando, M. Ohh, A. Salic, J.M. Asara, W.S. Lane, and W.J. Kaelin. 2001. HIFalpha targeted for VHL-mediated destruction by proline hydroxylation: implications for O_2 sensing. *Science* 292: 464–468.
47. Heidbreder, M., F. Frohlich, O. Johren, A. Dendorfer, F. Qadri, and P. Dominiak. 2003. Hypoxia rapidly activates HIF-3alpha mRNA expression. *FASEB Journal* 17: 1541–1543.
48. Zhang, P., Q. Yao, L. Lu, Y. Li, P.J. Chen, and C. Duan. 2014. Hypoxia-inducible factor 3 is an oxygen-dependent transcription activator and regulates a distinct transcriptional response to hypoxia. *Cell Reports* 6: 1110–1121.
49. Sarada, S., M. Titto, P. Himadri, S. Saumya, and V. Vijayalakshmi. 2015. Curcumin prophylaxis mitigates the incidence of hypobaric hypoxia-induced altered ion channels expression and impaired tight junction proteins integrity in rat brain. *Journal of Neuroinflammation* 12: 113.

50. Koh, H.S., C.Y. Chang, S. Jeon, H.J. Yoon, Y. Ahn, H. Kim, I. Kim, S.H. Jeon, R.S. Johnson, and E.J. Park. 2015. The HIF-1/glial TIM-3 axis controls inflammation-associated brain damage under hypoxia. *Nature Communications* 6: 6340.
51. Villa, P., P. Bigini, T. Mennini, D. Agnello, T. Laragione, A. Cagnotto, B. Viviani, M. Marinovich, A. Cerami, T.R. Coleman, M. Brines, and P. Ghezzi. 2003. Erythropoietin selectively attenuates cytokine production and inflammation in cerebral ischemia by targeting neuronal apoptosis. *Journal of Experimental Medicine* 198: 971–975.
52. Marti, H.H., R.H. Wenger, L.A. Rivas, U. Straumann, M. Digicaylioglu, V. Henn, Y. Yonekawa, C. Bauer, and M. Gassmann. 1996. Erythropoietin gene expression in human, monkey and murine brain. *European Journal of Neuroscience* 8: 666–676.
53. Masuda, S., M. Okano, K. Yamagishi, M. Nagao, M. Ueda, R. Sasaki. 1994. A novel site of erythropoietin production. Oxygen-dependent production in cultured rat astrocytes. *Journal of Biological Chemistry* 269: 19488–19493.
54. Rabie, T., and H.H. Marti. 2008. Brain protection by erythropoietin: a manifold task. *Physiology* 23: 263–274.